Synthesis, characterization and solid-state photoluminescence studies of six alkoxy phenylene ethynylene dinuclear palladium (II) rods.

João Figueira[a†], Wojciech Czardybon[a∩], José Carlos Mesquita[a], João Rodrigues[a]*, Fernando Lahoz[b]*, Luca Russo[c⊥], Arto Valkonen[c‖] and Kari Rissanen[c]*

[a]*CQM – Centro de Química da Madeira, MMRG, Universidade da Madeira, Campus Universitário da Penteada, 9000-390 Funchal, Portugal.*
[b]*Departamento de Física Fundamental y Experimental, Electrónica y Sistemas, Faculdad de Física, Universidad de La Laguna, 38206 La Laguna, Spain.*
[c]*Department of Chemistry, NanoScience Center, University of Jyväskylä, PO. Box 35, 40014 JYU, Finland.*

Present address: [†]Clinical Neuroscience Unit, Department of Pharmacology and Clinical Neuroscience, Umeå University, 90187 Umeå, Sweden. [∩] Selvita S.A. ul. Bobrzyńskiego 1430-348 Kraków, Poland. [⊥]Rigaku Europe SE, Am Hardtwald 11, 76275 Ettlingen, Germany. [‖] Tampere University of Technology, Department of Chemistry and Bioengineering, P. O. Box 541, 33101 Tampere, Finland

Supplementary Information

Table of contents

Figure index

Table index

1. Experimental details

The preparation of the tris ringed analogues of **1a** and **1d** (**4a** and **4d**) was burdened with isolation and purification problems and as such are not presented in this work (as well as the final longer complexes **7a** and **7d**). Nevertheless, the numbering was maintained to improve ease of comparison between the prepared analogues.

The preparation of the intermediaries (**2b-c** and **3b-c**) is described next. The method used for the synthesis of these compounds was already described on the main article and follows the Sonogashira-Hagihara coupling[1-10].

1.1. 1,4-dimethoxy-2,5-bis(4-bromophenyleethynyl)benzene, 2b

1,4-dimethoxy-2,5-diethynylbenzene (**1b**, 400 mg, 2.1 mmol), [$PdCl_2(PPh_3)_2$] (75 mg, 0.01 mmol), CuI (40 mg, 0.02 mmol), NEt_3 (20 mL), THF (20 mL), triphenylphosphine (28 mg, 0.01 mmol) and 1-bromo-4-iodobenzene (1.276 g, 4.5 mmol. Obtained a white powder (442 mg, 53.3 %).

^{1}H NMR (400 MHz, $CDCl_3$): δ 3.90 (*s*, 6H, OC*H*$_3$), 7.02 (*s*, Ar-*H*, central ring) 7.42 (*d*, 4H, Ar-*H* outer ring, $J_{H,H}$= 8.68 Hz), 7.49 (*d*, 4H, Ar-*H* outer ring, $J_{H,H}$ = 8.60 Hz) ppm.

1.2. 1,4-diethoxy-2,5-bis(4-bromophenyleethynyl)benzene, 2c

1,4-diethoxy-2,5-diethynylbenzene (**1c**, 876 mg, 4.1 mmol), [$PdCl_2(PPh_3)_2$] (143 mg, 0.2 mmol), CuI (77 mg, 0.41 mmol), NEt_3 (20 mL), THF (20mL) and 1-bromo-4-iodobenzene (3.471 g, 12.3 mmol. Obtained a white powder (816 mg, 38.1 %).

^{1}H NMR (400 MHz, $CDCl_3$): δ 1.47 (*t*, 6H, OC*H*$_2$CH$_3$), 4.11 (*q*, 4H, OC*H*$_2$CH$_3$), 7.01 (*s*, Ar-*H*, central ring) 7.40 (*d*, 4H, Ar-*H* outer ring, $J_{H,H}$= 8.48 Hz), 7.49 (*d*, 4H, Ar-*H* outer ring, $J_{H,H}$ = 8.73 Hz) ppm;

1.3. 1,4-dimethoxy-2,5-bis((4-trimethylsilylethynylphenyl)ethynyl)benzene, 3b

1,4-dimethoxy-2,5-bis(4-bromophenyleethynyl)benzene (**2b**, 3 g, 6 mmol), [$PdCl_2(PPh_3)_2$] (424 mg, 0.6 mmol), CuI (23 mg, 1.2 mmol), NEt_3 (30 mL), THF (30 mL) and trimethylsilylacetylene (1.31 g, 13.3 mmol. Obtained a yellow powder (1.16 g, 38.3 %).

^{1}H NMR (400 MHz, $CDCl_3$): δ 0.26 (*s*, 18H, Si(CH_3)$_3$), 3.90 (*s*, 6H, OCH_3), 7.02 (*s*, Ar-*H*, central ring) 7.44 (*d*, 4H, Ar-*H* outer ring, $J_{H,H}$= 8.32 Hz), 7.49 (*d*, 4H, Ar-*H* outer ring, $J_{H,H}$ = 8.32 Hz) ppm;

1.4. 1,4-diethoxy-2,5-bis((4-trimethylsilylethynylphenyl)ethynyl)benzene, 3c

1,4-diethoxy-2,5-bis(4-bromophenyleethynyl)benzene (**2c**, 1.165 g, 2.22 mmol), [$PdCl_2(PPh_3)_2$] (78 mg, 0.11 mmol), CuI (42 mg, 0.22 mmol), NEt_3 (30 mL), THF (30 mL) triphenylphosphine (58 mg, 0.22 mmol) and trimethylsilylacetylene (655 mg, 6.67 mmol. Obtained a yellow powder (667 mg, 53.7 %).

^{1}H NMR (400 MHz, $CDCl_3$): 0.26 (*s*, 18H, Si(CH_3)$_3$), δ 1.48 (*t*, 6H, OCH_2CH_3), 4.11 (*q*, 4H, OCH_2CH_3), 7.01 (*s*, Ar-*H*, central ring) 7.44 (*d*, 4H, Ar-*H* outer ring, $J_{H,H}$= 8.52 Hz), 7.47 (*d*, 4H, Ar-*H* outer ring, $J_{H,H}$ = 8.08 Hz) ppm;

2. Characterization

2.1. Absorption spectra

Table S. 1. Selected values for maximum the absorption peaks and their respective molar extinction coefficients for the free ligands (**1a-d**, **4b-c**), the palladium rods (**6a-d**, **7b-c**) and the free Pd complex (**5**).

Ligand	**λ_{max} (nm)**	**$\varepsilon \times 10^3$ $M^{-1}cm^{-1}$**	Complex	**λ_{max} (nm)**	**$\varepsilon \times 10^3$ $M^{-1}cm^{-1}$**
Shorter compounds					
1a	235 290	3 16	**6a**	232 277 314	16 19 27
1b	231 262 271 346	26 21 33 10	**6b**	238 283 302 362	25 27 33 31
1c	231 261 271 336	18 13 21 5	**6c**	238 273 302 353	26 29 35 31
1d	232 262 271 338	14 10 16 5	**6d**	237 274 283 302 351	25 26 26 32 25
Longer compounds					
4b	248 316 375	18 28 27	**7b**	237 275 333 385	22 22 25 42
4c	249 318 377	25 41 41	**7c**	236 275 336 385	18 17 20 35
Free starting complex					
			5	229 323	5 7

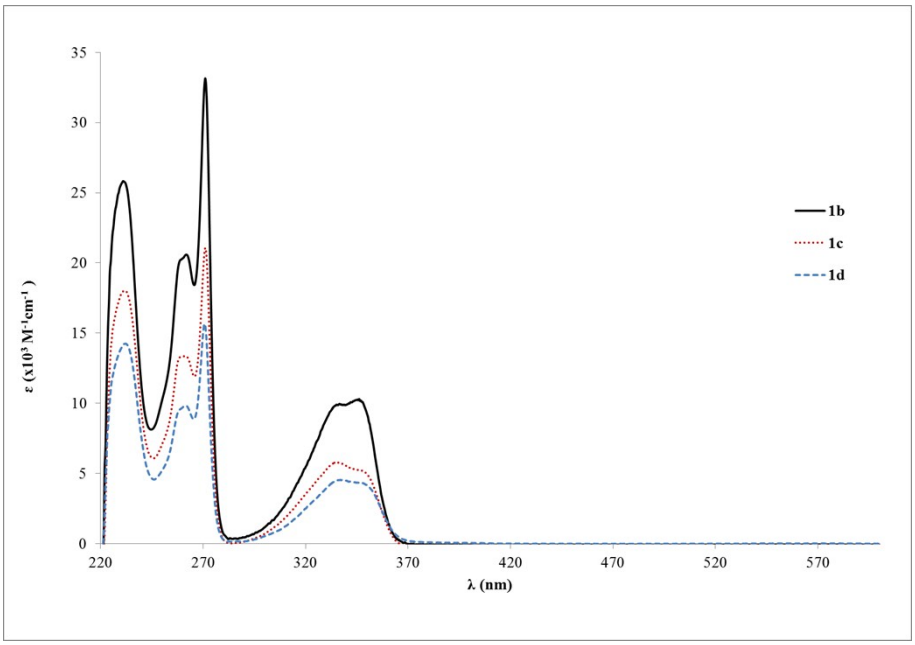

Fig. S. 1. Electronic spectra (ε *vs.* λ) for the shorter free ligands (**1b-d**) in CH_2Cl_2.

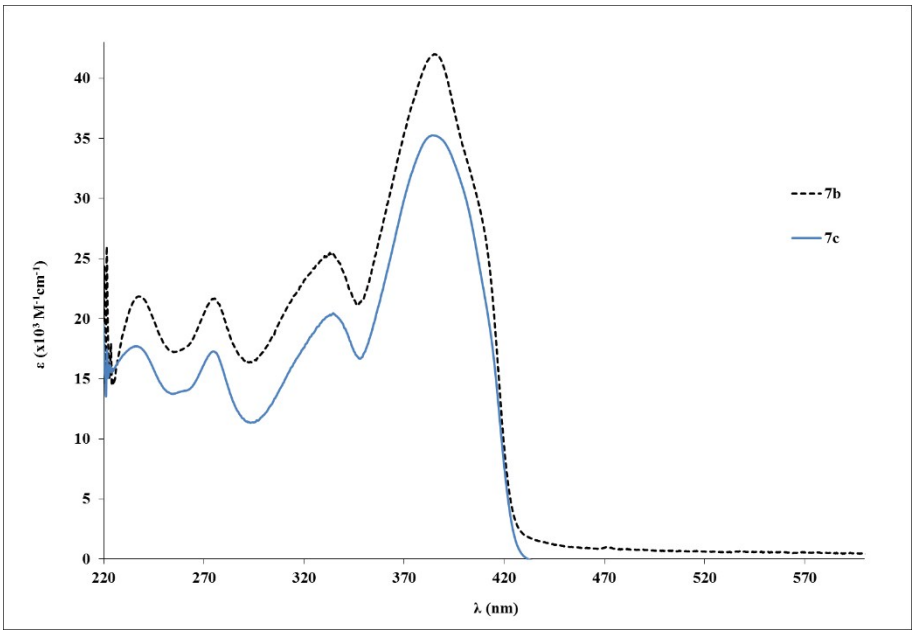

Fig. S. 2. Electronic spectra (ε *vs.* λ) for the longer rods (**7b-c**) in CH_2Cl_2.

2.2. FTIR Spectra

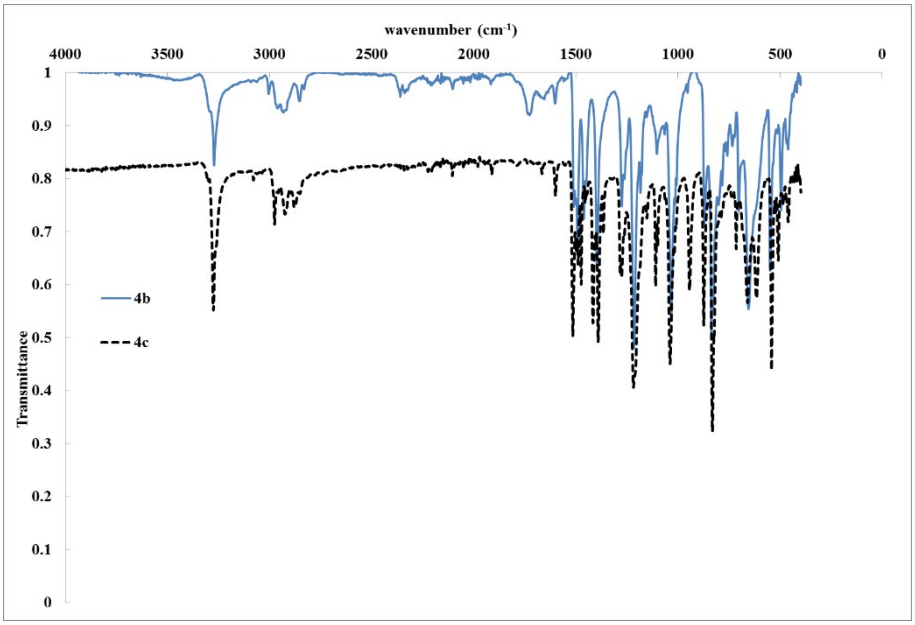

Fig. S. 3. FT-IR spectra for the tris ringed PE ligands (**4b-c**).

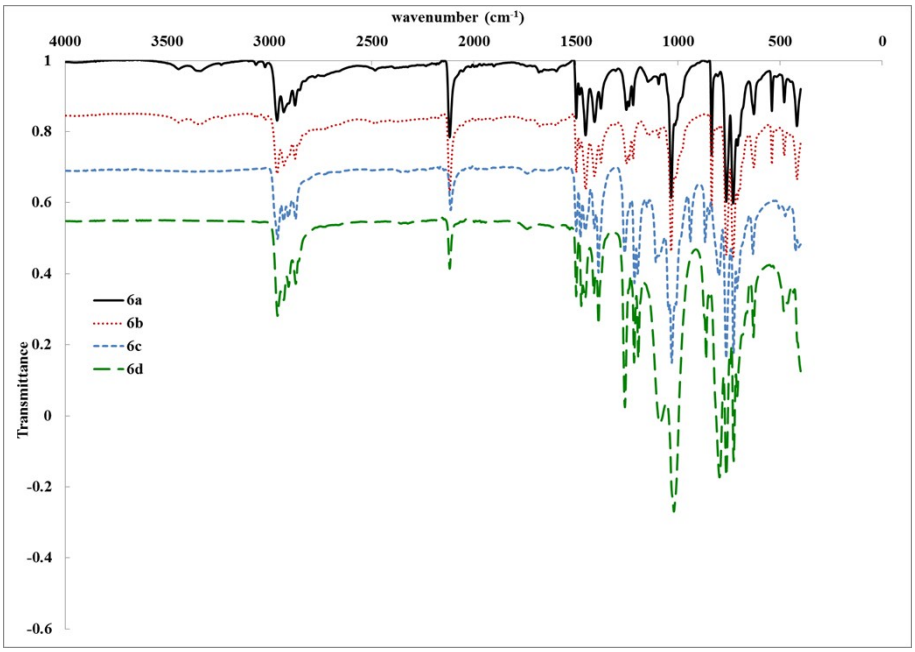

Fig. S. 4. FT-IR spectra for the single ringed PE based palladium rods (**6a-d**).

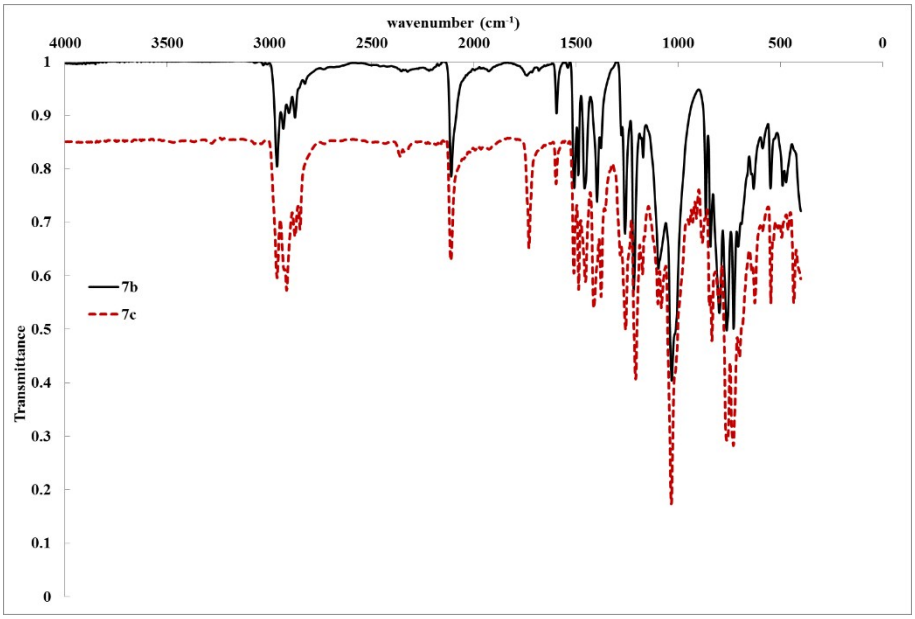

Fig. S. 5. FT-IR spectra for the tris ringed PE based palladium Rods (**7b-c**).

2.3. NMR spectra

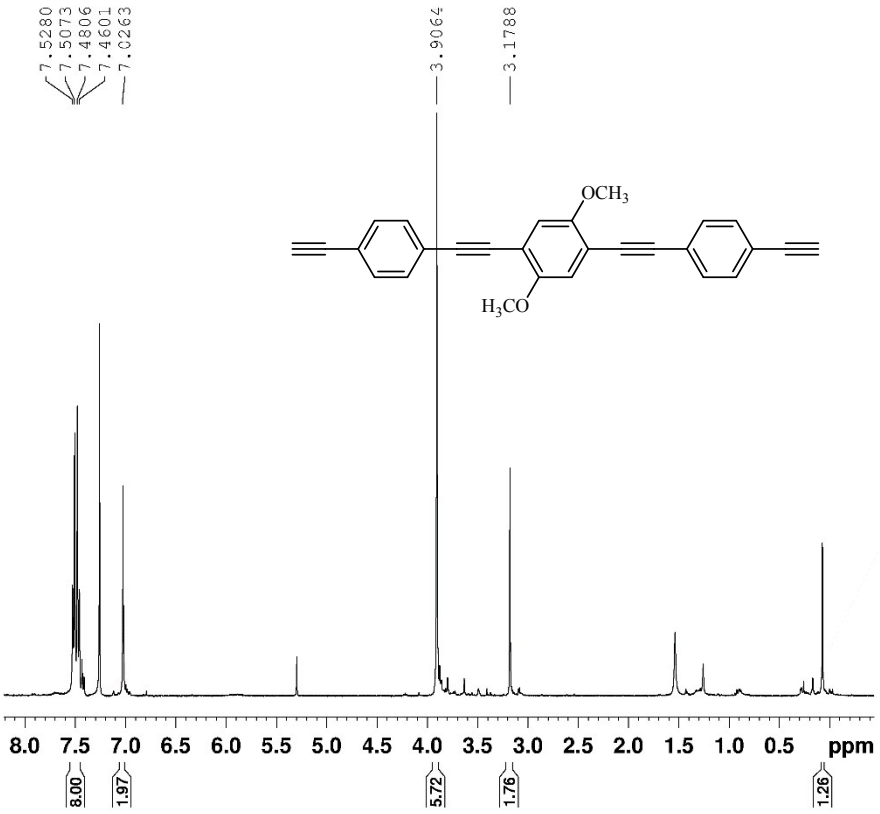

Fig. S. 6. ^{1}H NMR($CDCl_3$, 400MHz) spectrum of **4b**.

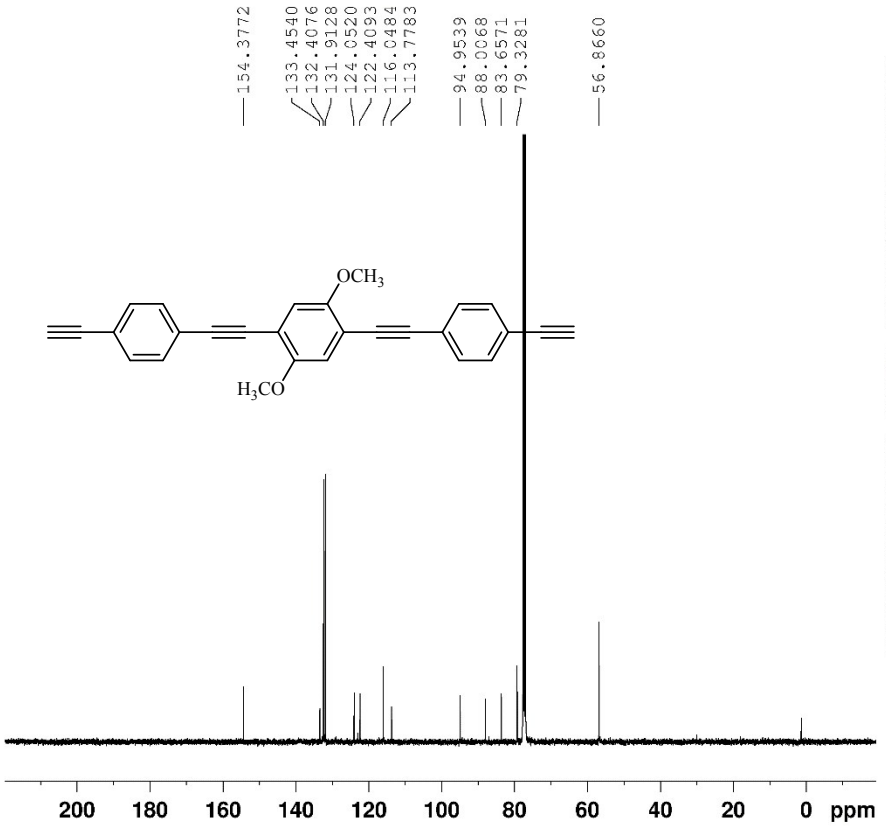

Fig. S. 7. $^{13}C\{^{1}H\}$ NMR($CDCl_3$, 101MHz) spectrum of **4b**.

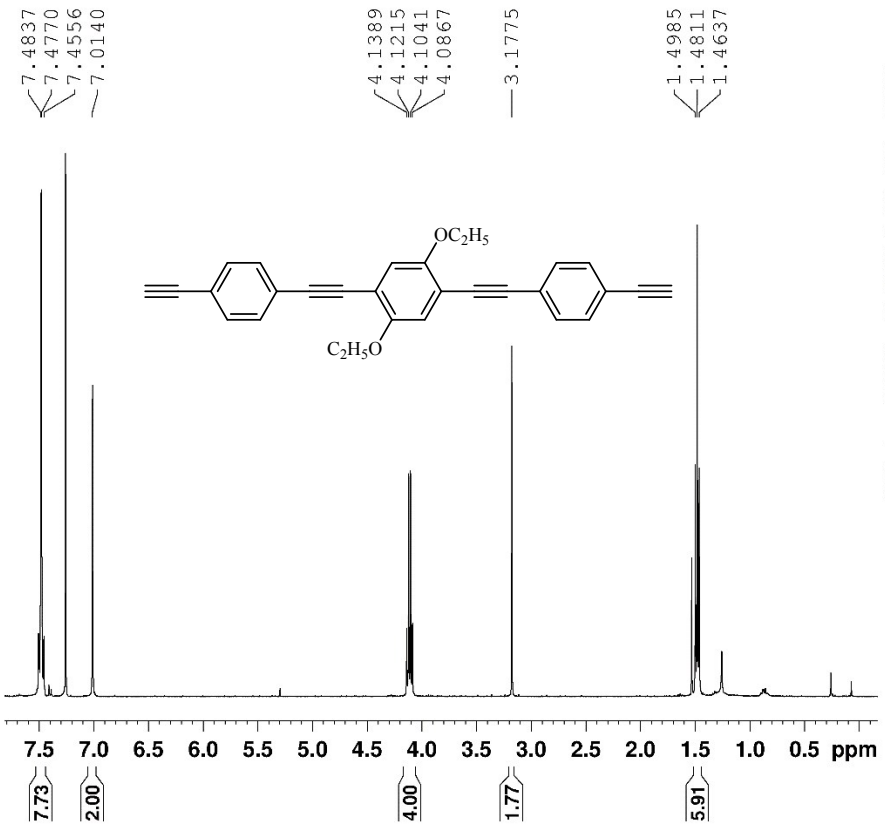

Fig. S. 8. ^{1}H NMR($CDCl_3$, 400MHz) spectrum of **4c**.

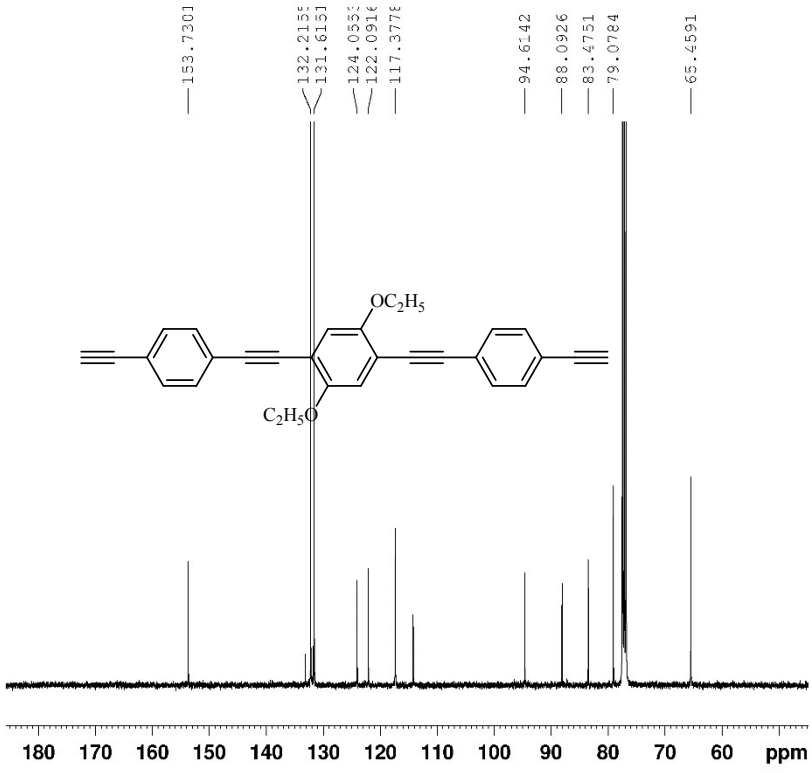

Fig. S. 9. $^{13}C\{^{1}H\}$ NMR($CDCl_3$, 101MHz) spectrum of **4c**.

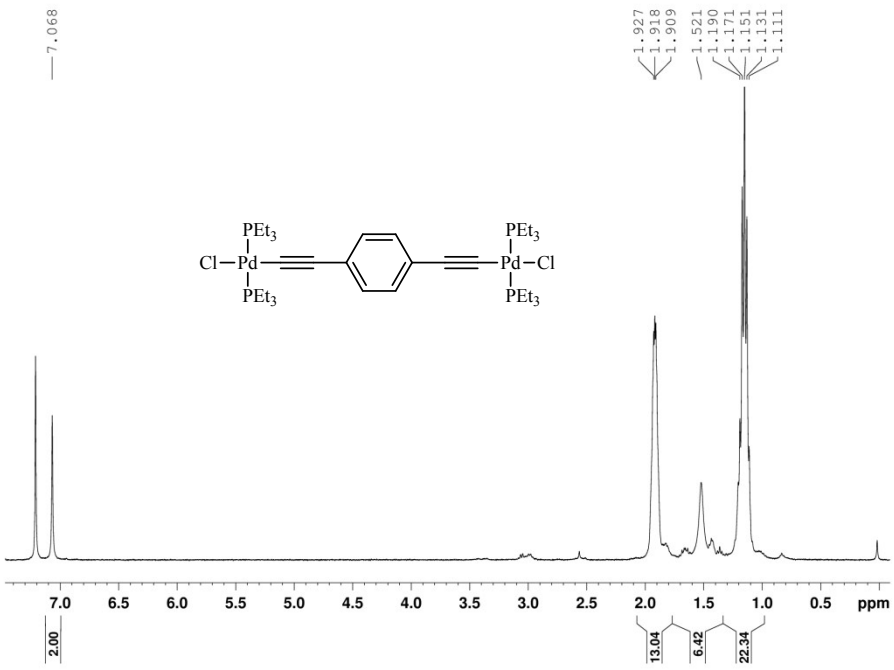

Fig. S. 10. ^{1}H NMR($CDCl_3$, 400MHz) spectrum of **6a**.

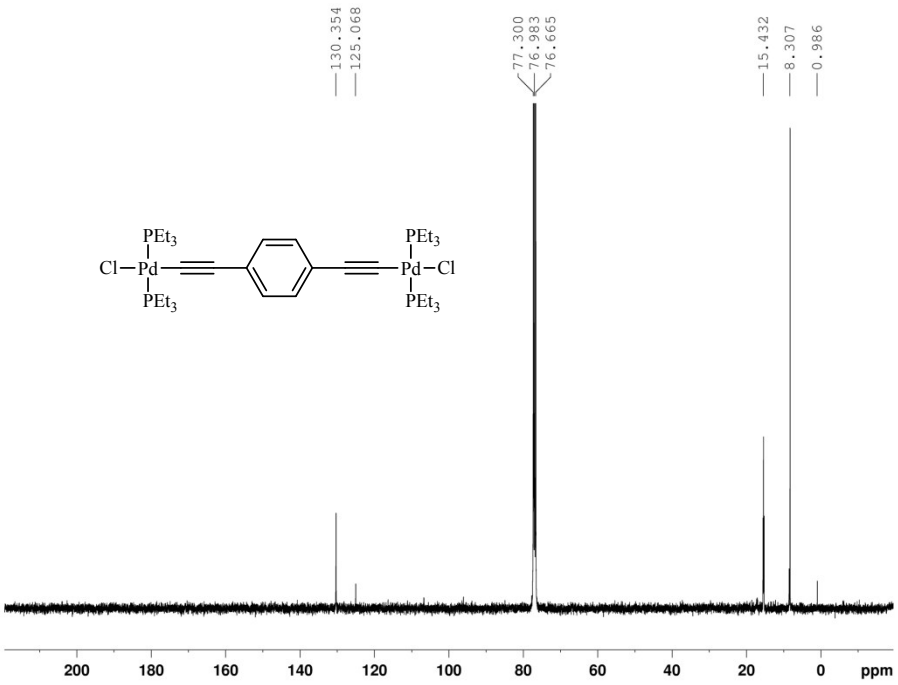

Fig. S. 11. $^{13}C\{^{1}H\}$ NMR($CDCl_3$, 101MHz) spectrum of **6a**.

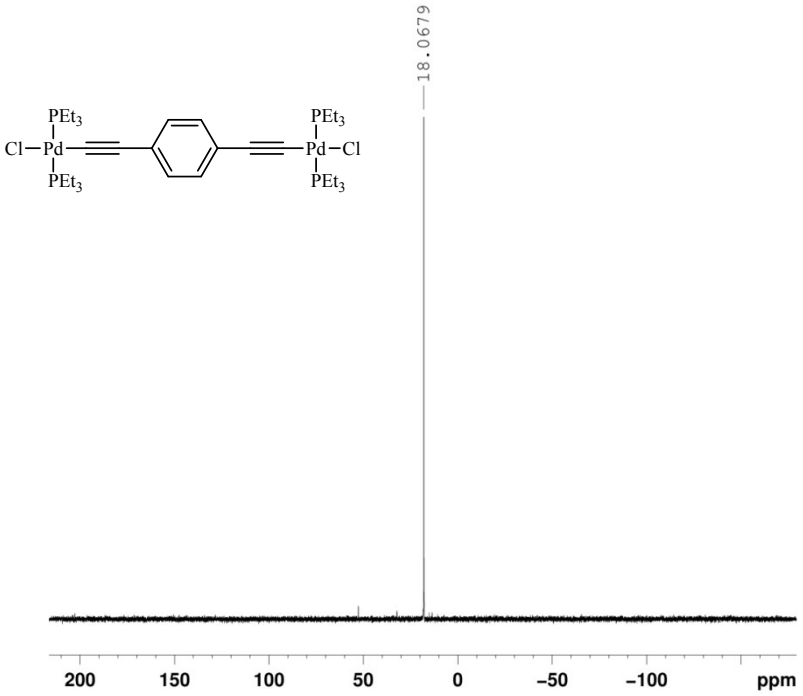

Fig. S. 12. $^{31}P\{^{1}H\}$ NMR($CDCl_3$, 161MHz) spectrum of **6a**.

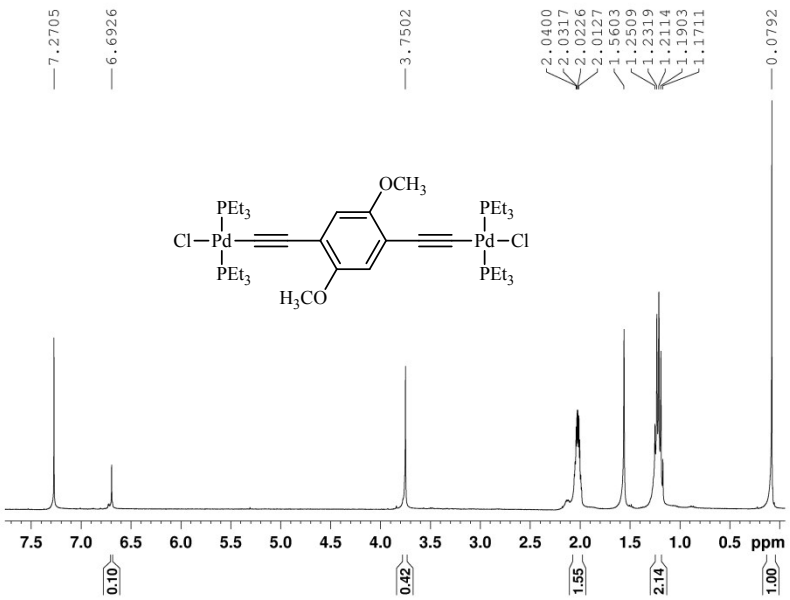

Fig. S. 13. ^{1}H NMR($CDCl_3$, 400MHz) spectrum of **6b**.

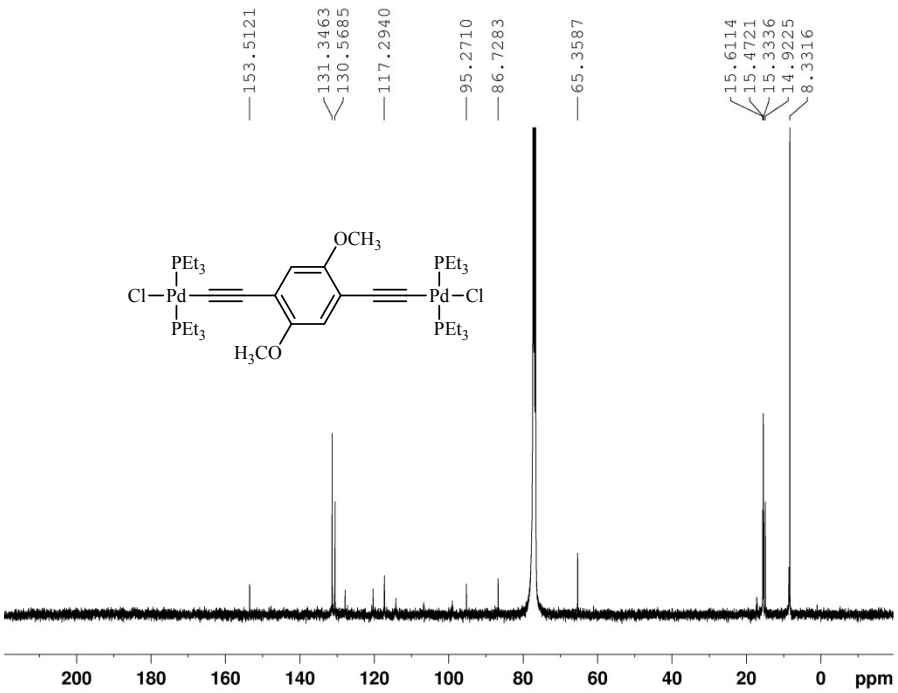

Fig. S. 14. $^{13}C\{^{1}H\}$ NMR($CDCl_3$, 101MHz) spectrum of **6b**.

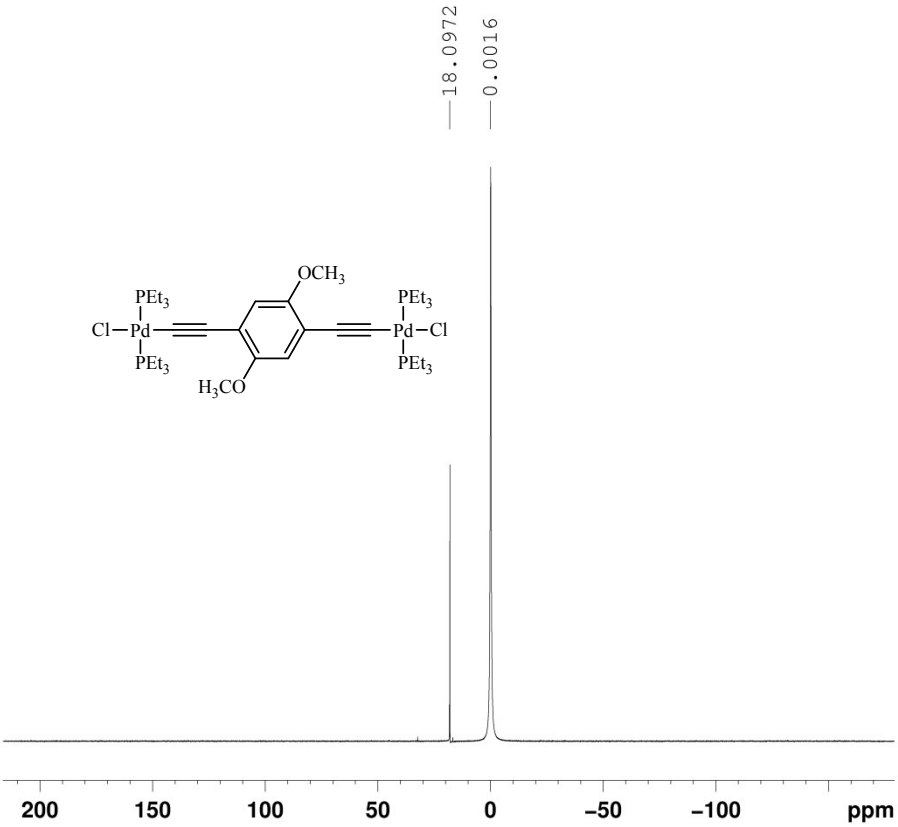

Fig. S. 15. $^{31}P\{^{1}H\}$ NMR($CDCl_3$, 161MHz) spectrum of **6b**.

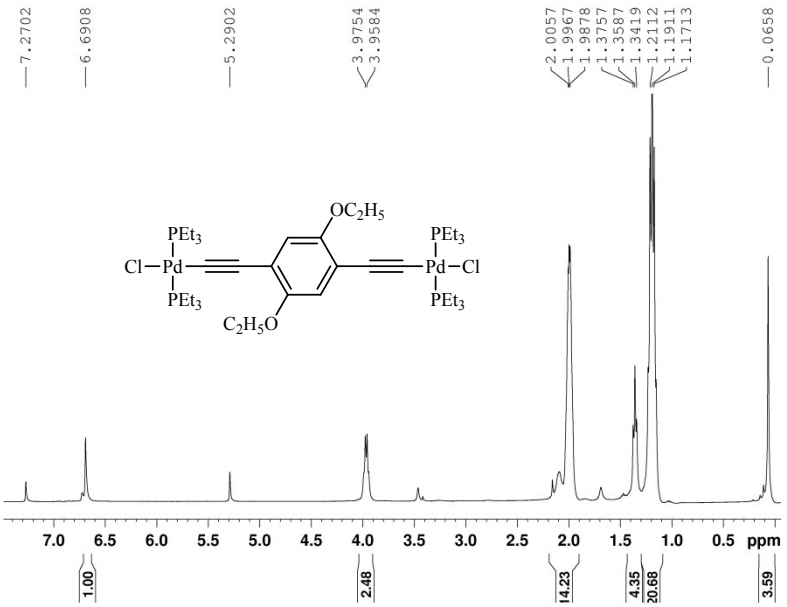

Fig. S. 16. ^{1}H NMR($CDCl_3$, 400MHz) spectrum of **6c**.

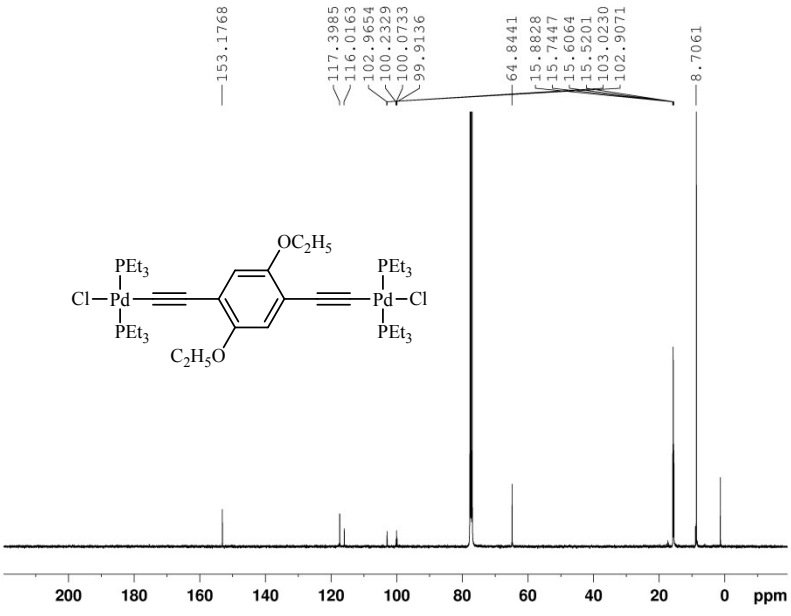

Fig. S. 17. $^{13}C\{^{1}H\}$ NMR($CDCl_3$, 101MHz) spectrum of **6c**.

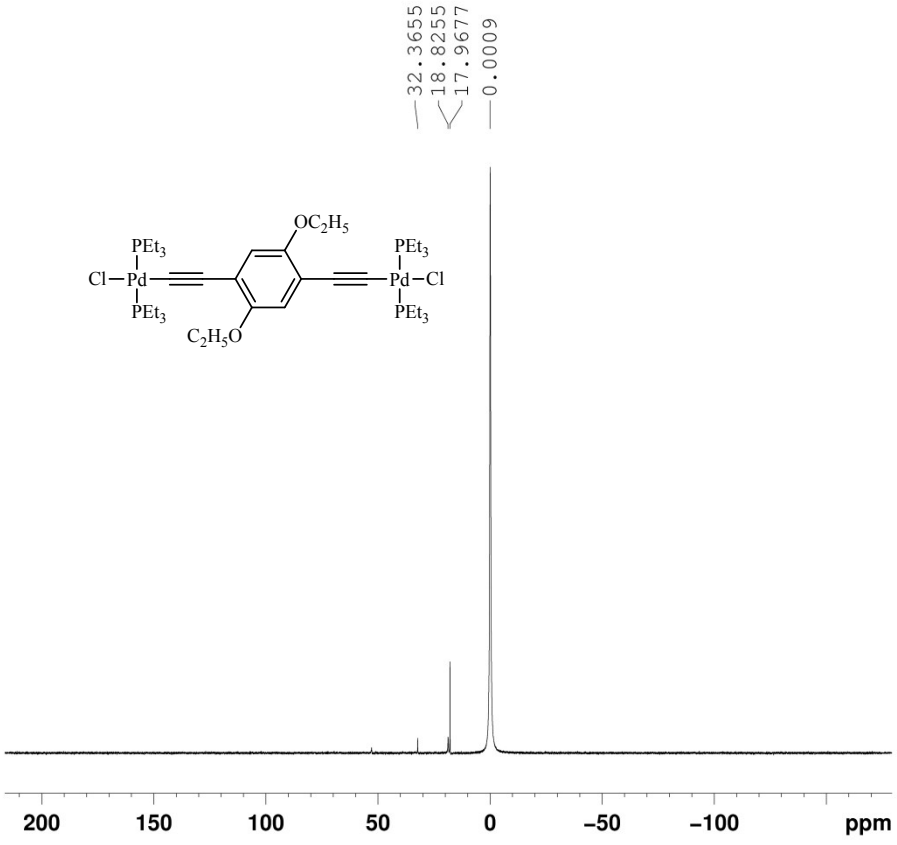

Fig. S. 18. $^{31}P\{^{1}H\}$ NMR($CDCl_3$, 161MHz) spectrum of **6c.**

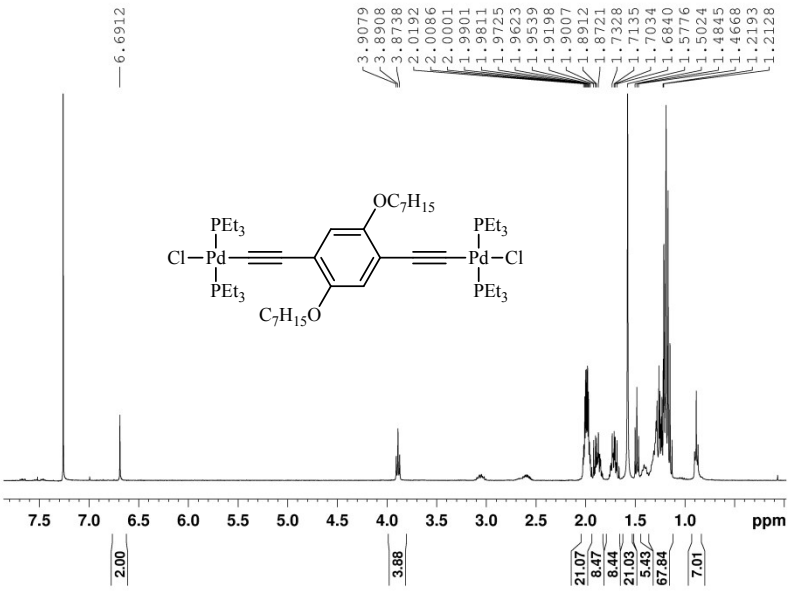

Fig. S. 19. ^{1}H NMR($CDCl_3$, 400MHz) spectrum of **6d**.

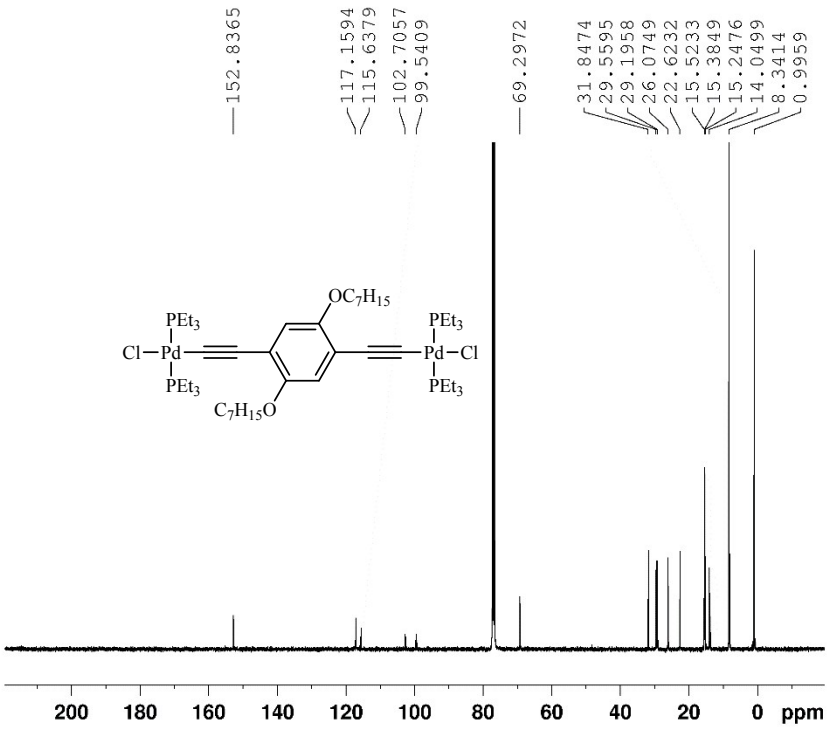

Fig. S. 20. $^{13}C\{^{1}H\}$ NMR($CDCl_3$, 101MHz) spectrum of **6d**.

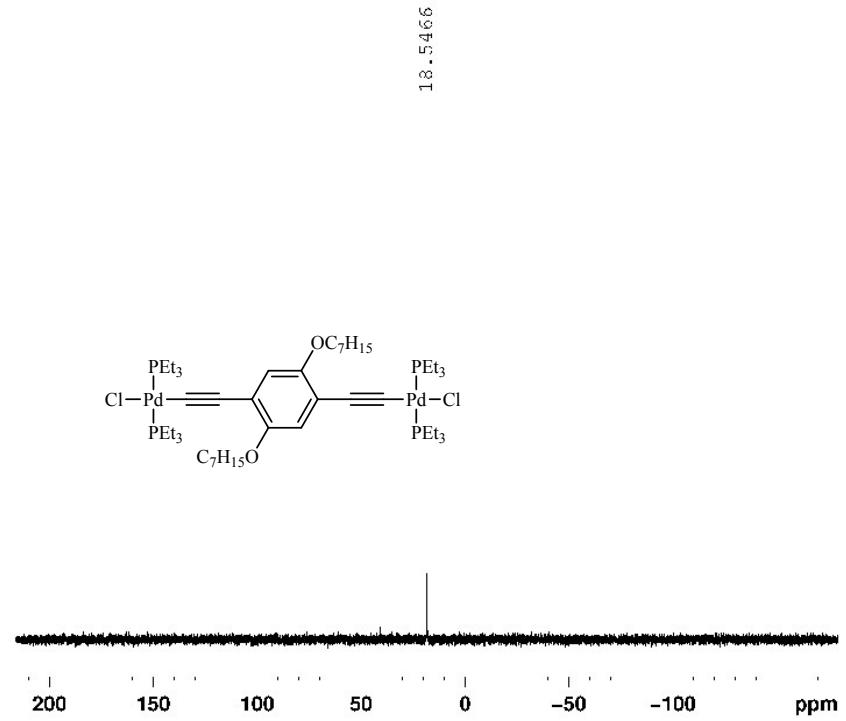

Fig. S. 21. $^{31}P\{^{1}H\}$ NMR($CDCl_3$, 161MHz) spectrum of **6d.**

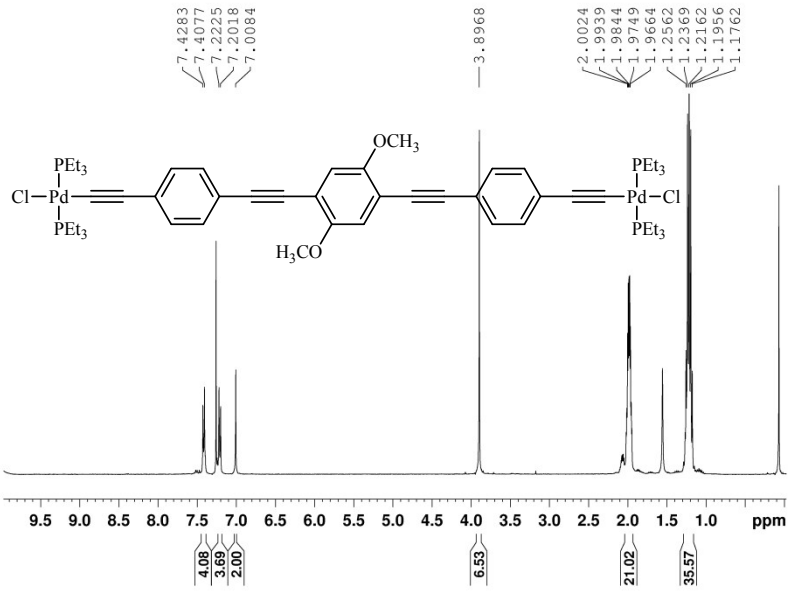

Fig. S. 22. ^{1}H NMR($CDCl_3$, 400MHz) spectrum of **7b**.

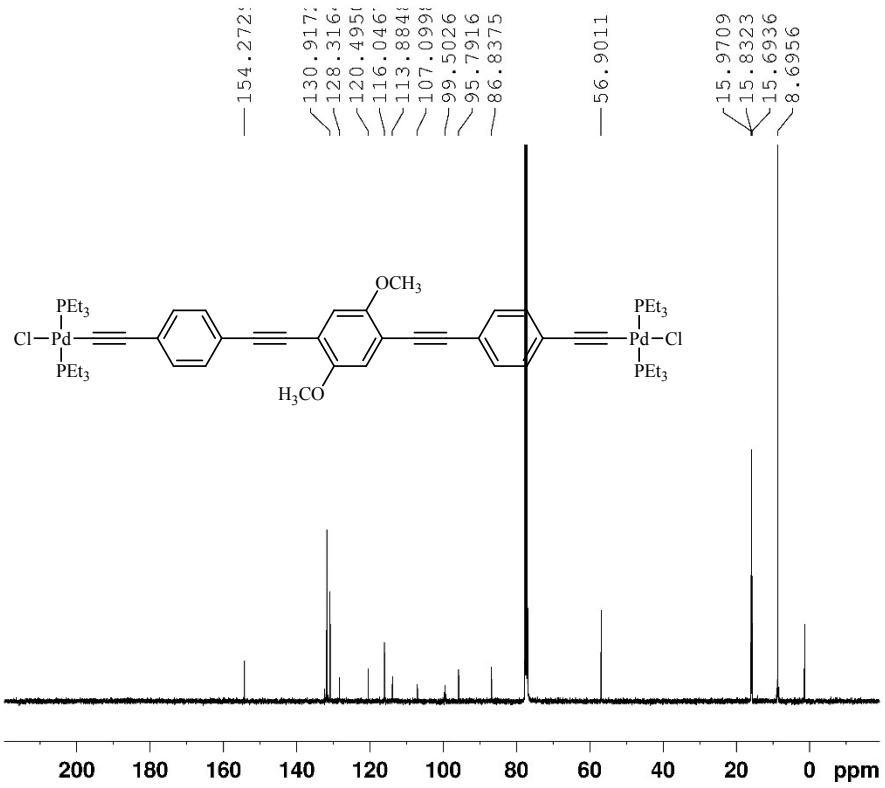

Fig. S. 23. $^{13}C\{^{1}H\}$ NMR($CDCl_3$, 101MHz) spectrum of **7b**.

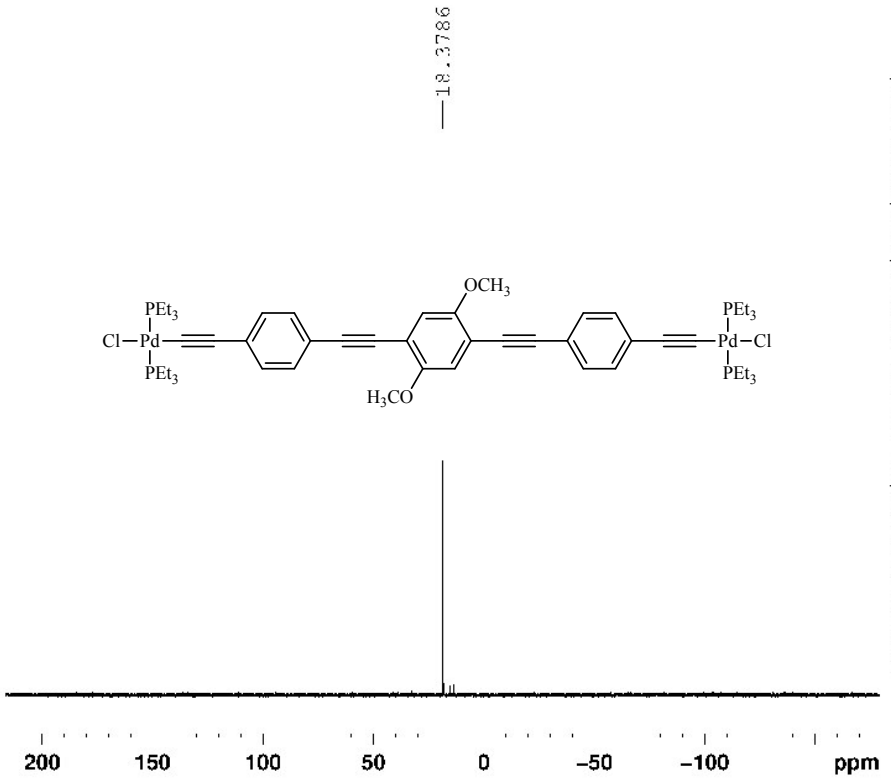

Fig. S. 24. $^{31}P\{^{1}H\}$ NMR($CDCl_3$, 161MHz) spectrum of **7b**.

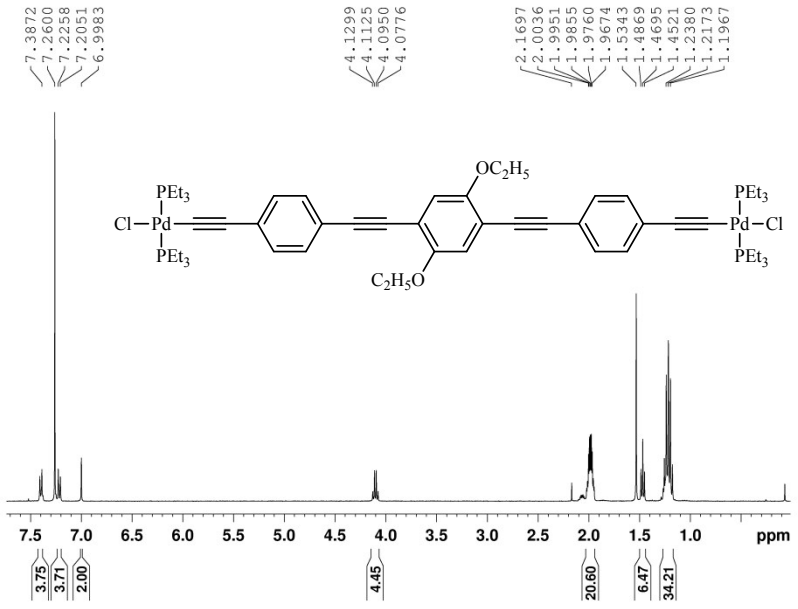

Fig. S. 25. ^{1}H NMR($CDCl_3$, 400MHz) spectrum of **7c**.

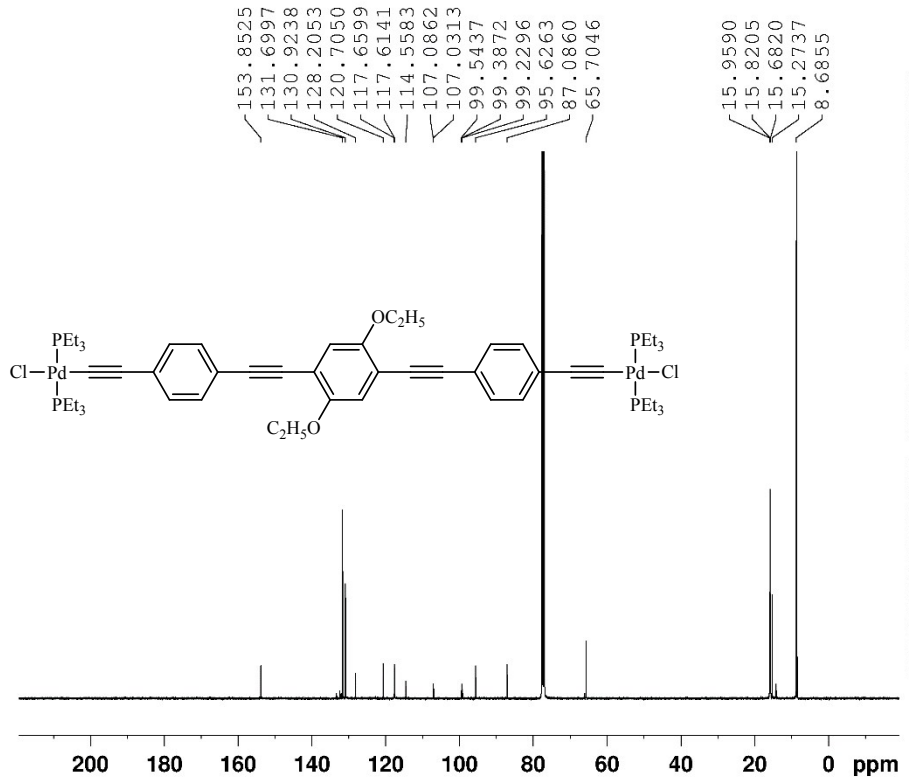

Fig. S. 26. $^{13}C\{^{1}H\}$ NMR($CDCl_3$, 101MHz) spectrum of **7c**.

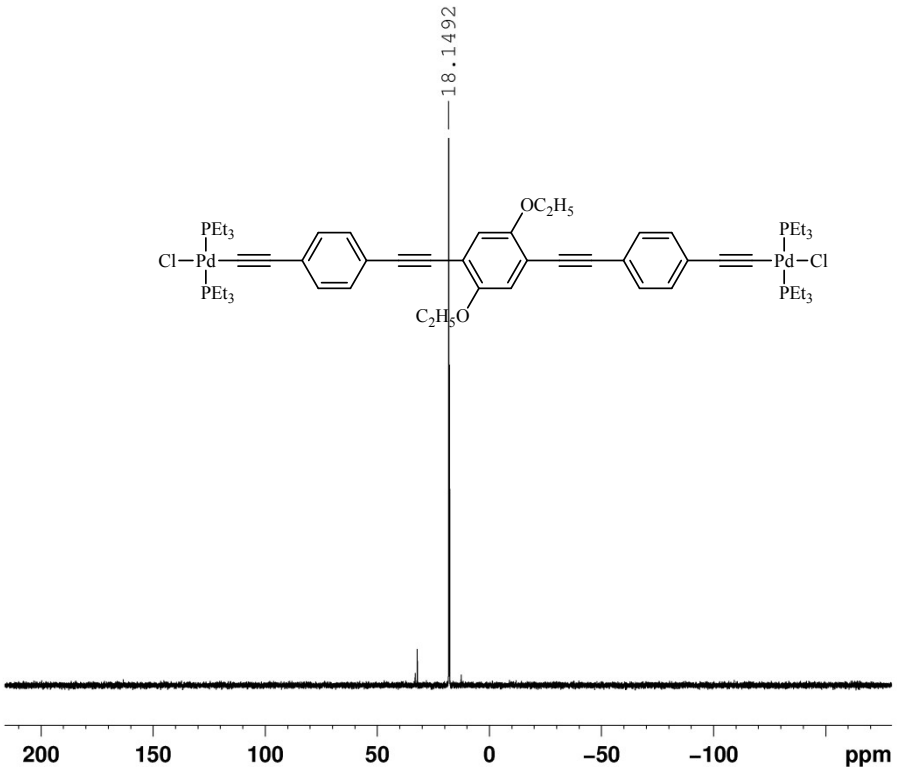

Fig. S. 27. $^{31}P\{^{1}H\}$ NMR($CDCl_3$, 161MHz) spectrum of **7c.**

2.4. Cyclic voltammetry

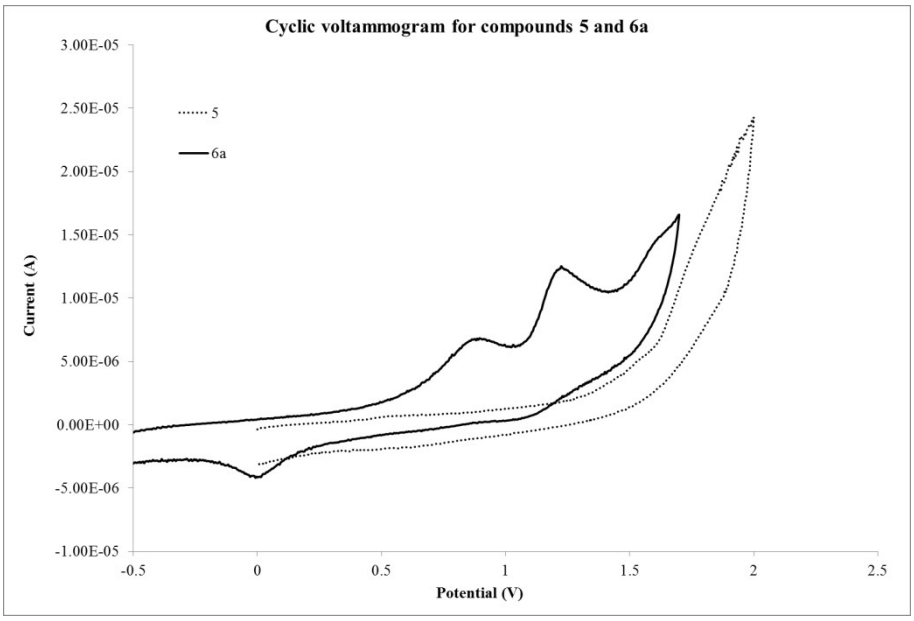

Fig. S. 28. Cyclic voltammograms for compounds **5** and **6a** at 100 mVs^{-1} *vs.* Ag/AgCl (KCl saturated) in CH_2Cl_2.

2.5. MS spectra

The MS spectra which resulted from ESI-TOF analysis are presented in this section.

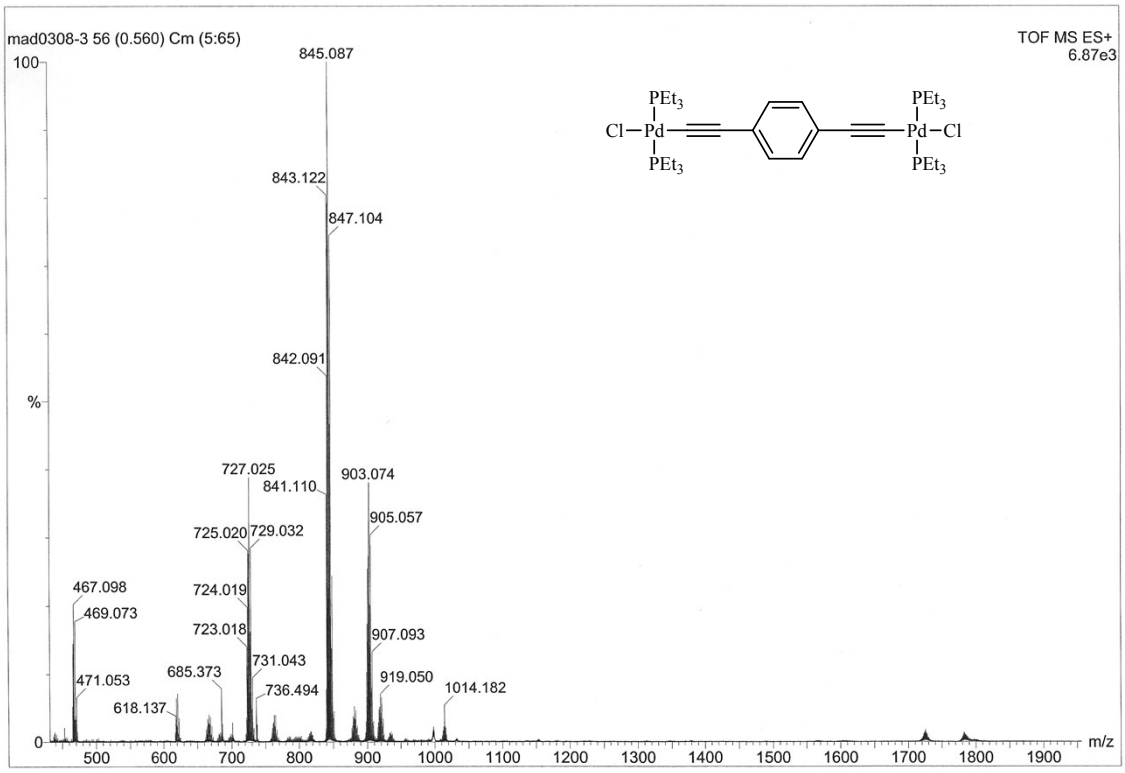

Fig. S. 29. ESI-MS(TOF+) spectrum of **6a**.

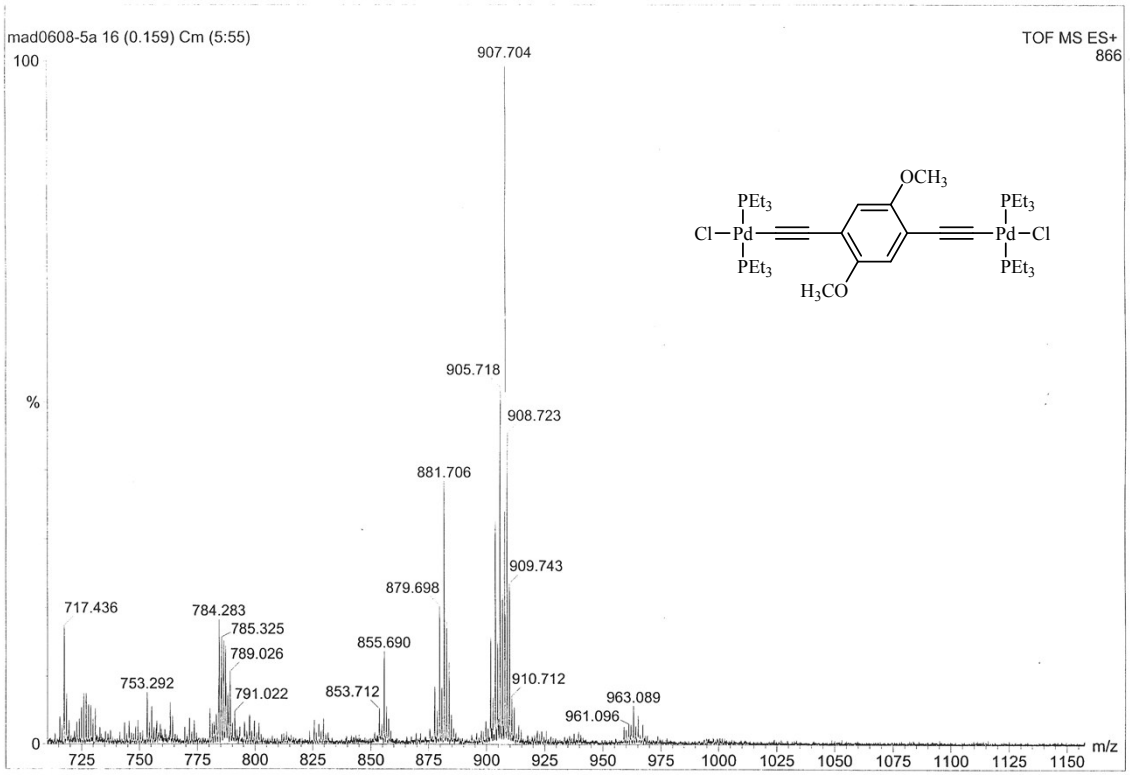

Fig. S. 30. ESI-MS(TOF+) spectrum of **6b**.

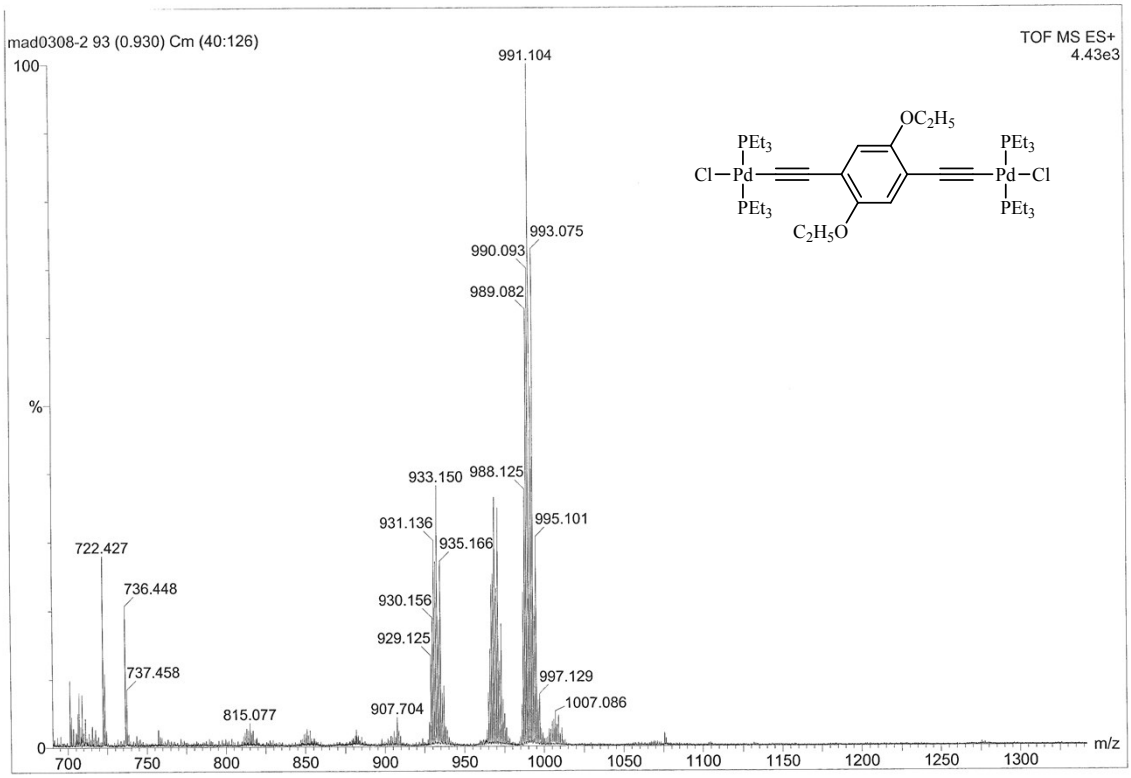

Fig. S. 31. ESI-MS(TOF+) spectrum of **6c**.

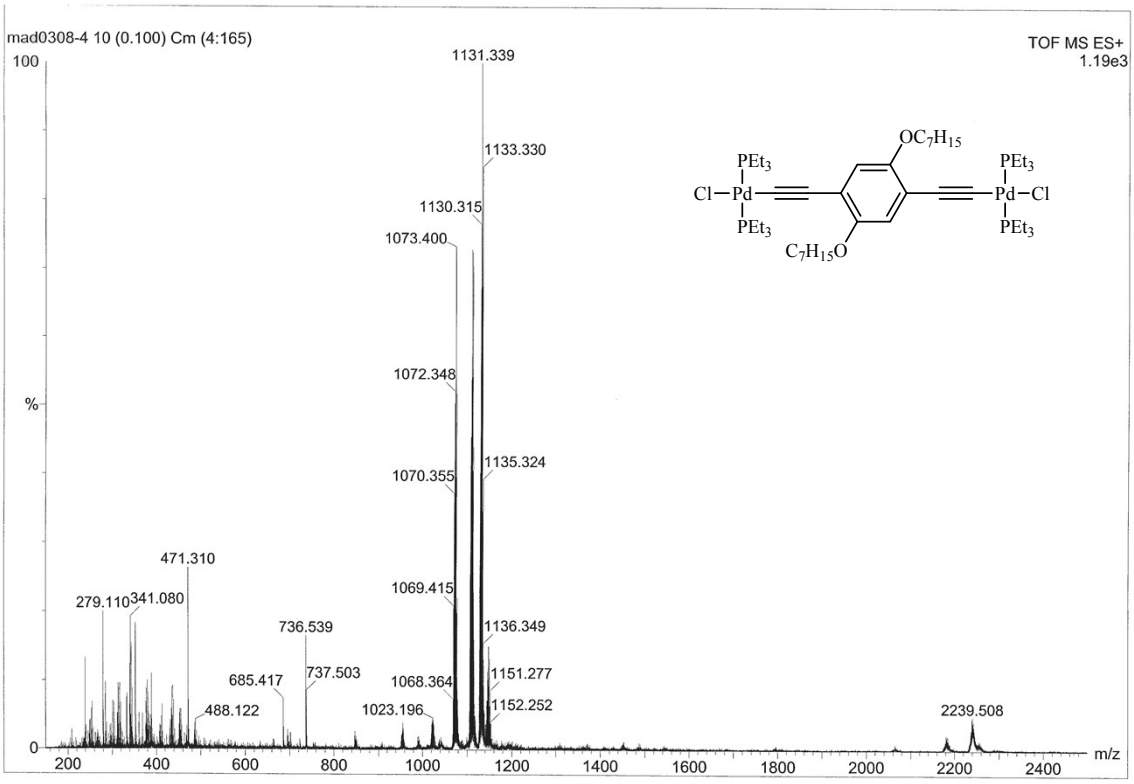

Fig. S. 32. ESI-MS(TOF+) spectrum of **6d**.

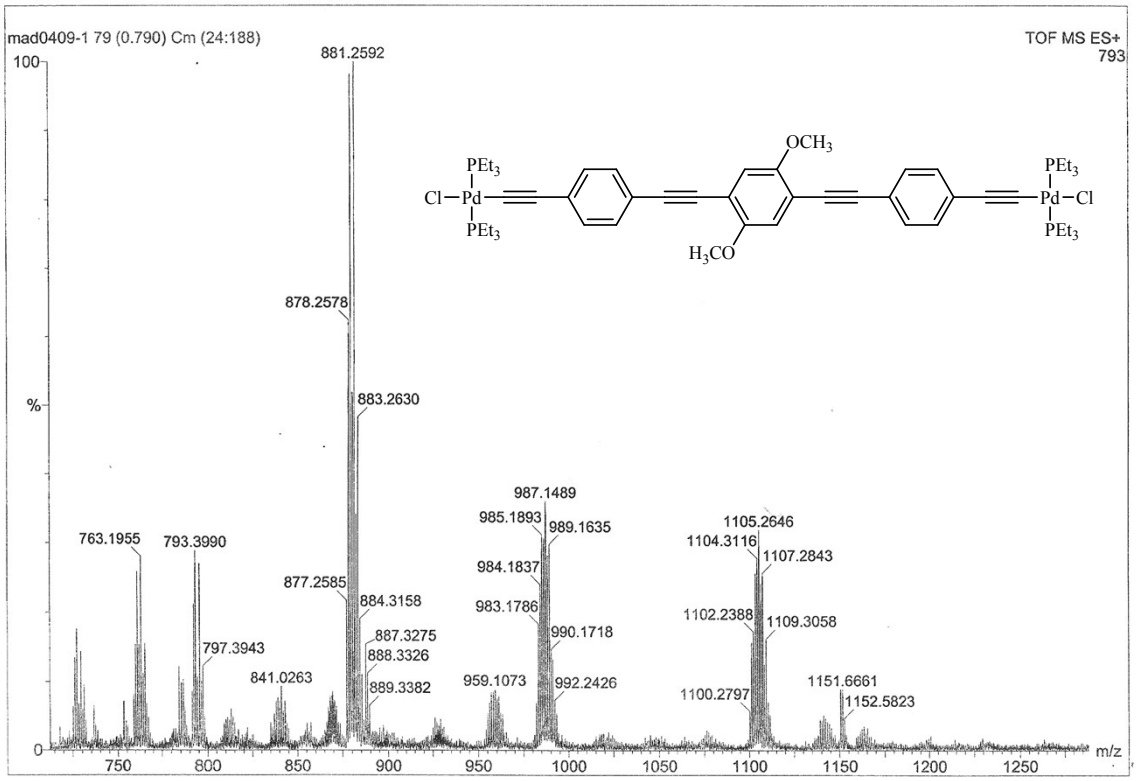

Fig. S. 33. ESI-MS(TOF+) spectrum of **7b**.

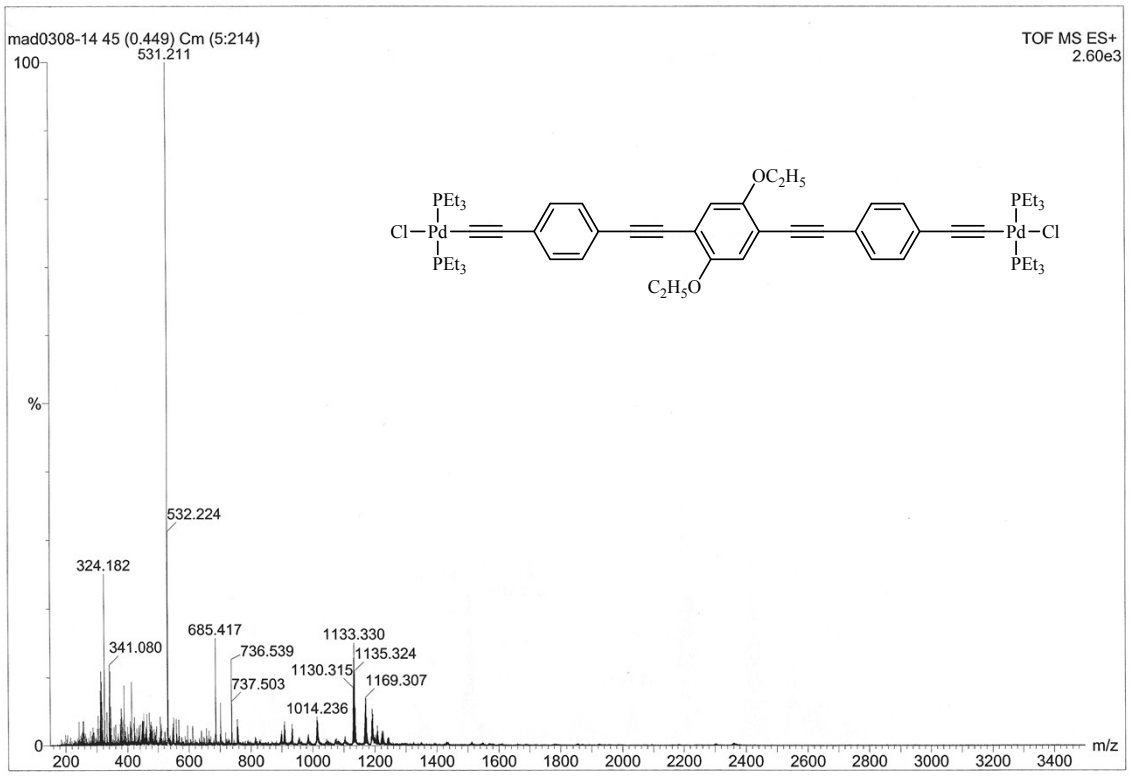

Fig. S. 34. ESI-MS(TOF+) spectrum of **7c**.

2.6. X-ray crystal structures

Table S. 2. Selected bond distances (Å) and angles (º) for the structures of **6c** and **7c**.[#]

6c		**7c**	
Pd1 – Cl1	2.362(2)	Pd1 – Cl1	2.346(6) [2.384(10)]
Pd1 – P1	2.320(2)	Pd1 – P1	2.283(7) [2.336(8)]
Pd1 – P8	2.320(2)	Pd1 – P2	2.340(4) [2.306(7)]
Pd1 – C15	1.965(7)	Pd1 – C13	1.947(6)
C15 – C16	1.176(9)	C13 – C12	1.184(8)
C16 – C17	1.469(9)	C12 – C9	1.444(8)
C17 – C18	1.410(9)	C1 – C2	1.405(9)
C18 – O20	1.385(7)	C2 – O1	1.360(8)
C18 – C19	1.385(8)	C2 – C3	1.398(8)
O20 – C21	1.433(8)	O1 – C26	1.436(8)
		C4 – C5	1.200(8)
		C6 – C5	1.430(8)
		C1 – C4	1.429(8)
P1 – Pd1 – Cl1	88.18(7)	P1 – Pd1 – Cl1	96.5(2)
P8 – Pd1 – Cl1	96.14(7)	P2 – Pd1 – Cl1	89.1(2)
P1 – Pd1 – P8	175.66(8)	P1 – Pd1 – P2	171.1(2)
C15 – Pd1 – Cl1	177.0(2)	C13 – Pd1 – Cl1	177.8(2)
C16 – C15 – Pd1	176.0(7)	C12 – C13 – Pd1	178.1(6)
C17 – C16 – C15	175.0(8)	C13 – C12 – C9	177.0(7)
O20 – C18 – C19	124.3(6)	O1 – C2 – C3	125.3(6)
		C5 – C4 – C1	175.9(7)
		C4 – C5 – C6	176.8(7)
C4 – O1 – C6	116.1(5)	C2 – O1 – C26	118.6(5)

[#]Distances of minor component in brackets

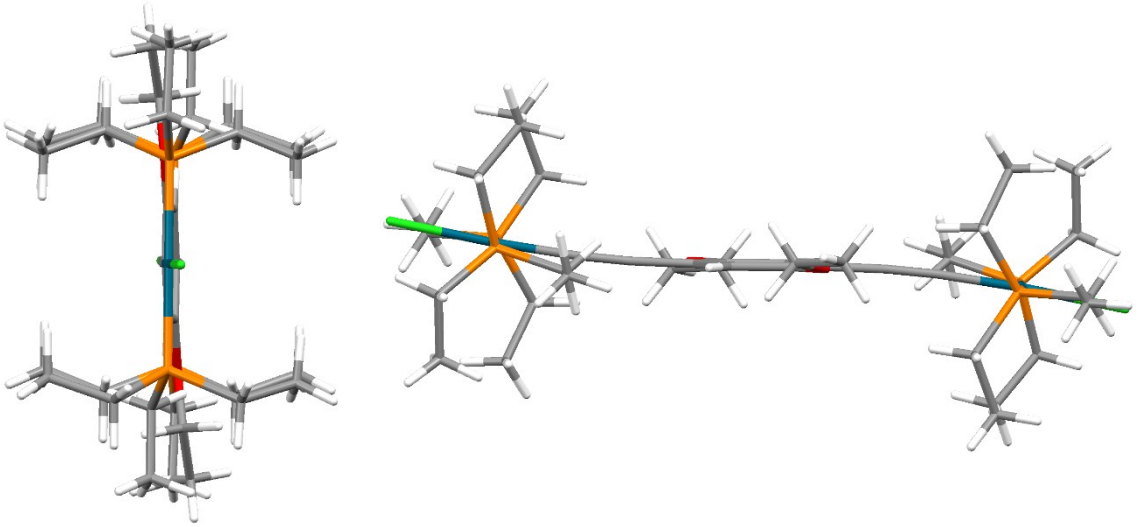

Fig. S. 35. Two Mercury[11] views of molecule **6c**. The view on the left shows the molecule along Pd–Pd axis with central phenylene placed in vertical orientation. It illustrates the almost co-planar behavior of Pd coordination plane and central aryl ring. Inside view (on the right) of the molecule, the central phenylene is drawn horizontal.

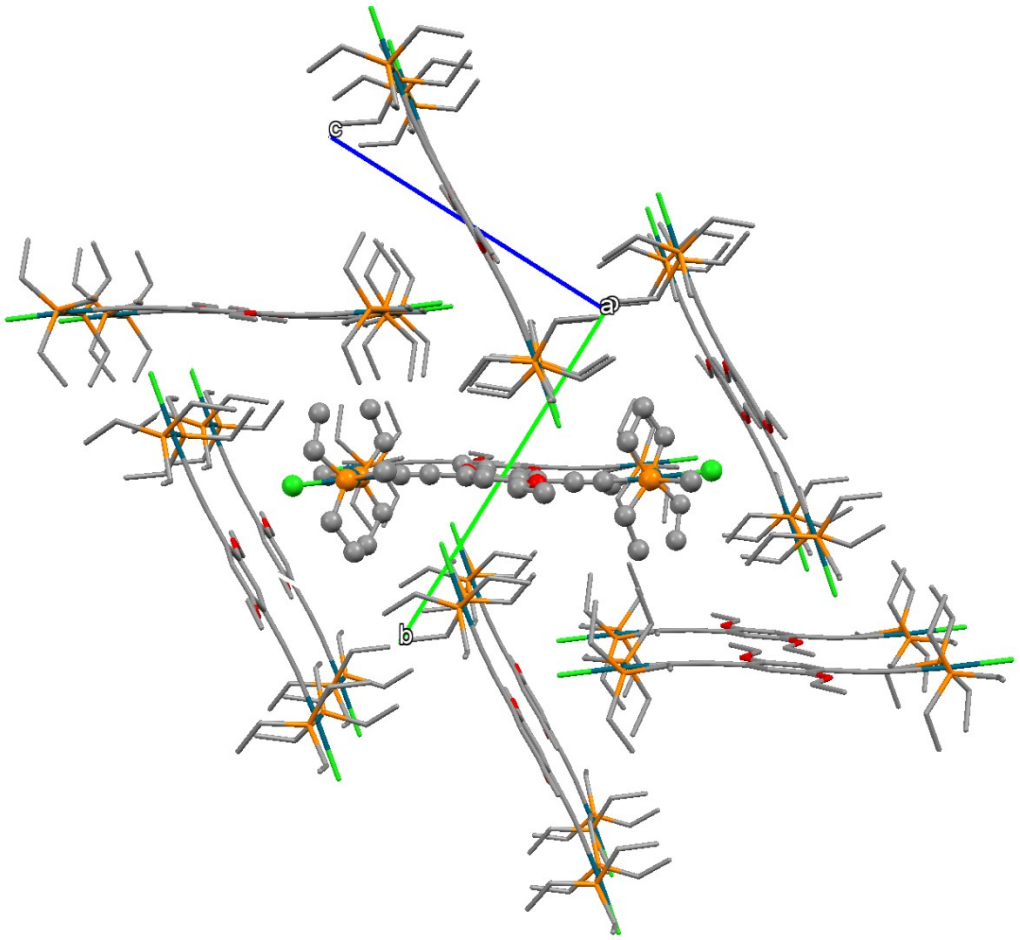

Fig. S. 36. A packing diagram of **6c** (viewed along the *a*-axis) shows side-by-side pairs, which are actually forming an infinite chains along the *a*-axis. The molecule in asymmetric unit is emphasized (ball-and-stick), and hydrogen atoms are removed for clarity.

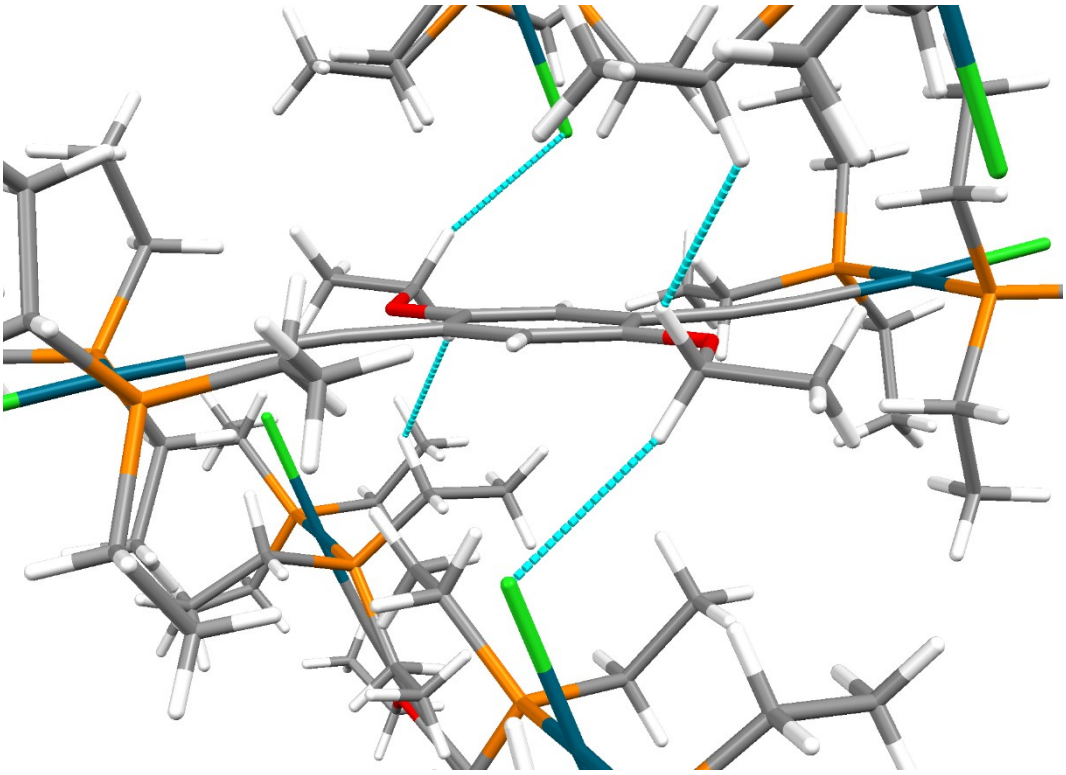

Fig. S. 37. A view from **6c**, which illustrates the packing short contacts found by Mercury[11] potentially influencing the ethoxy group orientations. Only two types of contacts were found and involved both methylene protons of ethoxy group: the potentially attractive C−H···Cl interaction (C···Cl 3.70 Å, H···Cl 2.80 Å, C−H···Cl 153°) and weakly repulsive H···H contact (H···H 2.35 Å). Still, they may bend the ethoxy groups out of the plane of core aryl ring.

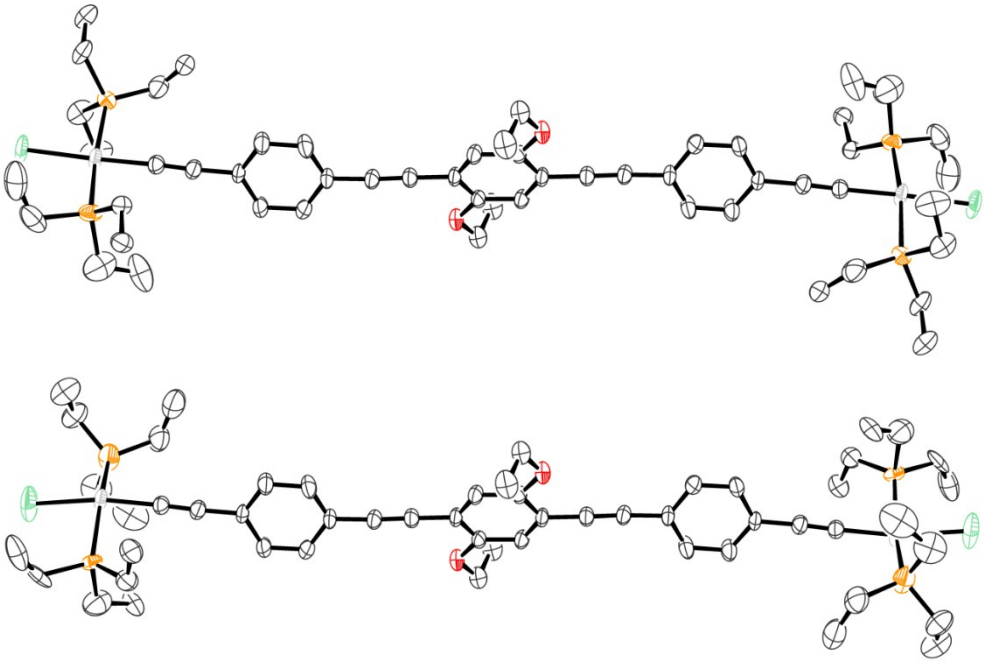

Fig. S. 38. ORTEP[12] plots of major (above) and minor (below) components of **7c**, showing the different spatial orientation of chlorines and -$P(Et)_3$ groups (ellipsoid probability 50 %).

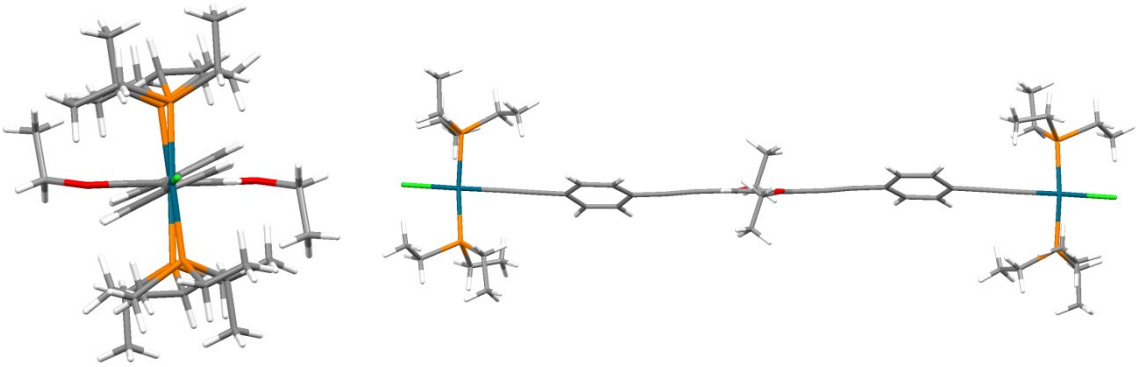

Fig. S. 39. Two Mercury[11] views of the major component of **7c** with central phenyl placed in horizontal orientation. The view on the left is showing the molecule along Pd–Pd axis and illustrating the almost perpendicular direction of Pd–P bonds. On the right, there is a side view with better outlook of the different orientation of aromatic moieties.

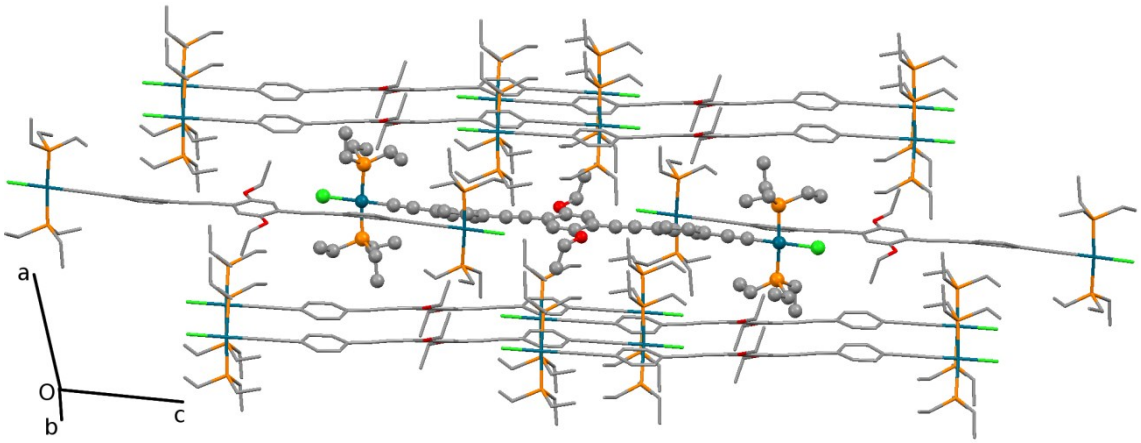

Fig. S. 40. A packing diagram of **7c**, where the molecule in asymmetric unit is emphasized (ball-and-stick). The molecules are forming laminar structure where every second sheet is showing a different orientation of molecules. The disorder and hydrogen atoms are removed for clarity.

3. References

1. O. Lavastre, J. Plass, P. Bachmann, S. Guesmi, C. Moinet and P. H. Dixneuf, *Organometallics*, 1997, **16**, 184-189.
2. S. M. Dirk, D. W. Price, S. Chanteau, D. V. Kosynkin and J. M. Tour, *Tetrahedron*, 2001, **57**, 5109-5121.
3. J. M. Tour, *Molecular Electronics: Commercial Insights, Chemistry, Devices, Architecture, and Programming*, World Scientific, River Edge, N.J., 2003.
4. U. H. F. Bunz, *Chem. Rev.*, 2000, **100**, 1605-1644.

5. X. H. Wu, S. Jin, J. H. Liang, Z. Y. Li, G.-a. Yu and S. H. Liu, *Organometallics*, 2009, **28**, 2450-2459.
6. K. L. Chandra, S. Zhang and C. B. Gorman, *Tetrahedron*, 2007, **63**, 7120-7132.
7. J. Figueira, J. Rodrigues, L. Russo and K. Rissanen, *Acta Crystallogr., Sect. C: Cryst. Struct. Commun.*, 2008, **64**, o33-o36.
8. K. Sonogashira, Y. Tohda and N. Hagihara, *Tetrahedron Lett.*, 1975, **16**, 4467-4470.
9. C. Weder and M. S. Wrighton, *Macromolecules*, 1996, **29**, 5157-5165.
10. A. Nagy, Z. Novák and A. Kotschy, *J. Organomet. Chem.*, 2005, **690**, 4453-4461.
11. C. F. Macrae, I. J. Bruno, J. A. Chisholm, P. R. Edgington, P. McCabe, E. Pidcock, L. Rodriguez-Monge, R. Taylor, J. van de Streek and P. A. Wood, *J. Appl. Crystallogr.*, 2008, **41**, 466-470.
12. L. J. Farrugia, *J. Appl. Crystallogr.*, 2012, **45**, 849-854.